



Cite this: *J. Mater. Chem. B*, 2015, 3, 5005

Received 16th January 2015,  
Accepted 10th March 2015

DOI: 10.1039/c5tb00106d

[www.rsc.org/MaterialsB](http://www.rsc.org/MaterialsB)

We report the preparation and characterization of films of electroactive supramolecular polymers based on non-electroactive oligoalanines and electroactive oligoanilines. Fibroblasts adhered to and proliferated on the films, and the delivery of the clinically relevant anti-inflammatory drug dexamethasone phosphate could be enhanced upon the application of an electrical stimulus.

Technologies that enable precise control of the amount of drugs in the blood stream or specific tissues facilitate the maintenance of the amount of drug within the therapeutic window, and controlling the chronopharmacology of a drug is particularly useful for the treatment of diseases with specific chronobiologies (e.g. cancers, infectious diseases, pain).<sup>1–3</sup> Drug delivery systems that respond to chemical (e.g. enzymes, pH) or physical (e.g. electric/magnetic fields, light, pH, temperature) stimuli are potentially applicable for the treatment of such conditions.<sup>2,3</sup> Here we report the application of electroactive polymers (EAPs) that allow drug delivery enhanced by the application of an electrical stimulus.

EAPs have interesting electronic and optical properties and are currently investigated for use in electronic<sup>4</sup> and biomedical<sup>5–8</sup> industries. Polyaniline, polypyrrole and polythiophene derivatives are the EAPs most commonly investigated for biomedical applications.<sup>9,10</sup> In recent years block copolymers incorporating electroactive blocks (frequently oligoaniline-based polymers doped with camphorsulfonic acid, CSA, Fig. 1) have been investigated for

## Peptide-directed assembly of functional supramolecular polymers for biomedical applications: electroactive molecular tongue-twisters (oligoalanine–oligoaniline–oligoalanine) for electrochemically enhanced drug delivery†

John G. Hardy,<sup>\*ab</sup> Megan N. Amend,<sup>b</sup> Sydney Geissler,<sup>ab</sup> Vincent M. Lynch<sup>c</sup> and Christine E. Schmidt<sup>\*ab</sup>

use as electroactive tissue scaffolds capable of the electrical stimulation of the cells inhabiting them,<sup>11</sup> and as materials for electrochemically-triggered drug delivery.<sup>12</sup>

Polyaniline- and polypyrrole-based systems have been used to deliver a variety of drugs, including; adenosine triphosphate, dexamethasone phosphate (DMP, Fig. 1), DNA, dopamine, nerve growth factor and *N*-methylphenothiazine, as discussed in greater depth in reviews by Garg and co-workers<sup>13</sup> and Ndesendo and co-workers.<sup>14</sup> Here we report the application of electroactive molecular tongue-twisters (MTTs) based on electroactive oligoanilines and non-electroactive oligoalanines (*i.e.* oligoalanine–oligoaniline–oligoalanine) for the delivery of dexamethasone phosphate. The MTTs are solution processable and assemble into hierarchically structured supramolecular polymers<sup>15–21</sup> because of hydrogen bonding interactions between the oligoalanines in the solid state. Such supramolecular polymers have prospects for the preparation of conformal electroactive coatings for implantable biomaterials.

The electrochemically responsive blocks of oligoaniline were terminated with amines which enabled the initiation of ring-opening polymerization of  $\alpha$ -amino acid *N*-carboxyanhydrides,<sup>22</sup> in this case alanine *N*-carboxyanhydride (Ala-NCA). The oligoanilines (tetraaniline and hexaaniline) were prepared using the methodology described in the literature (Scheme S1, ESI†),<sup>23,24</sup> as was Ala-NCA (Scheme S2, ESI†),<sup>25</sup> and they were polymerized at room temperature in anhydrous DMF, precipitated in diethyl ether and dried under vacuum (Scheme 1). The hexafluoroisopropanol

<sup>a</sup> Department of Biomedical Engineering, The University of Texas at Austin, Austin, TX 78712, USA

<sup>b</sup> J. Crayton Pruitt Family Department of Biomedical Engineering, University of Florida, Biomedical Sciences Building JG-53, P.O. Box 116131, Gainesville, FL 32611-6131, USA. E-mail: [johnhardyuk@gmail.com](mailto:johnhardyuk@gmail.com), [schmidt@bme.ufl.edu](mailto:schmidt@bme.ufl.edu)

<sup>c</sup> Department of Chemistry, The University of Texas at Austin, Austin, TX 78712, USA

† Electronic supplementary information (ESI) available: Full experimental details, synthetic schemes, FTIR spectra, XRD spectra, voltammograms, cell adhesion assay data, image of HDFs on TCP control substrate. See DOI: [10.1039/c5tb00106d](https://doi.org/10.1039/c5tb00106d)

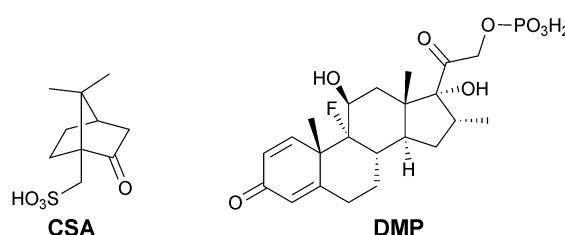
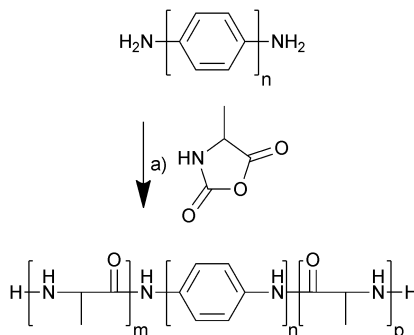


Fig. 1 Camphorsulfonic acid (CSA) and dexamethasone phosphate (DMP).





**Scheme 1** Synthesis of molecular tongue-twisters (oligoalanine–oligoaniline–oligoalanine) from alanine *N*-carboxyanhydrides and amine-terminated oligoanilines. (a) DMF, Ar, 96 h. For tetraaniline-based MTT1,  $n = 2$ , and  $m + p \approx 10$ ; whereas for hexaaniline-based MTT2,  $n = 4$ , and  $m + p \approx 26$ .

(HFIP)-soluble fraction was extracted and dried under vacuum, yielding off-white solids that were used without further purification; tetraaniline-based molecular tongue-twister 1 (MTT1, oligoalanine–tetraaniline–oligoalanine) and hexaaniline-based molecular tongue-twister 2 (MTT2, oligoalanine–hexaaniline–oligoalanine), that are depicted in Scheme 1.

The success of the polymerizations was confirmed spectroscopically. The presence of characteristic peaks in the IR spectra (Fig. S1, ESI<sup>†</sup>) for amides and oligoanilines (shoulders at *ca.* 1541 cm<sup>−1</sup> (C=N and C=C stretches) and 1496 cm<sup>−1</sup> (C=C stretching)).<sup>26</sup> NMR in deuterated HFIP suggested that MTT1 incorporated *ca.* 10 alanine units per tetraaniline (in line with the synthesis), whereas MTT2 incorporated 26 alanine units per hexaaniline, suggesting that polymers based on the less soluble hexaaniline required a greater number of alanines for the resulting polymer to be soluble. Yet their low solubility hampered determination of the molecular weight distributions *via* standard techniques such as GPC/SEC, light scattering or MALDI-TOF mass spectrometry.

Casting dilute solutions of the MTTs in HFIP allowed the preparation of water insoluble films of a few  $\mu\text{m}$  in thickness with  $\mu\text{m}$  scale roughness ( $R_a$ ) or root mean square roughness ( $R_q$ ) as determined by profilometry (Table 1). Undoped films were blue, whereas films doped with CSA (10 wt%) were green.

IR spectra of the films recorded in attenuated total reflectance (ATR) mode revealed subtle differences in the hierarchical supramolecular assembly of the polymers, with evidence of both  $\alpha$ -helices and  $\beta$ -sheets in all spectra (Fig. S1, ESI<sup>†</sup>),<sup>27–29</sup> with the  $\alpha$ -helices induced by HFIP and the intermolecular  $\beta$ -sheets being partially responsible for the insolubility of the polymers

in water (also observed in oligoalanine-rich proteins).<sup>30–32</sup> The oligoalanine blocks in undoped films of MTT1 assembled into both  $\alpha$ -helices (amide I, 1649 cm<sup>−1</sup>) and  $\beta$ -sheets (amide I, 1692 cm<sup>−1</sup>; amide II, 1530 and 1517 cm<sup>−1</sup>). Doping MTT1 with CSA altered the assembly of the MTTs, yet both  $\alpha$ -helices (amide I, 1649 cm<sup>−1</sup>; amide II, 1543 cm<sup>−1</sup>) and  $\beta$ -sheets (amide I, 1690 cm<sup>−1</sup>; amide II, 1530 and 1514 cm<sup>−1</sup>) were present, although the  $\beta$ -sheet content was clearly reduced. The oligoalanine blocks in undoped films of MTT2 were predominantly amorphous (amide I, 1646 cm<sup>−1</sup>; amide II, 1533 cm<sup>−1</sup>) with some  $\beta$ -sheets (amide I, 1629 cm<sup>−1</sup>; amide II, 1518 cm<sup>−1</sup>). Doping MTT2 with CSA reduced the  $\beta$ -sheet content (weak amide I, 1690 cm<sup>−1</sup>; weak amide II, 1530 and 1514 cm<sup>−1</sup>), and the chains were predominantly amorphous (amide I, 1646 cm<sup>−1</sup>; amide II, 1535 cm<sup>−1</sup>).<sup>27–29</sup>

Wide angle XRD patterns for the films (Fig. S2, ESI<sup>†</sup>) supported the results from IR spectroscopy, which showed evidence of both  $\alpha$ -helices (broad peak at  $2\theta = 19.4^\circ$ , *d*-spacing 4.58 Å) and  $\beta$ -sheets (broad peak at  $2\theta = 16.7^\circ$  and  $19.9^\circ$ , *d*-spacings of 5.31 and 4.46 Å, respectively) also observed in oligoalanine-rich proteins.<sup>29</sup> Films composed of MTT1 showed some peaks reported for tetraaniline-based supramolecular polymers (peaks at  $2\theta = 11.7^\circ$ ,  $19.5^\circ$ ,  $20.3^\circ$ ,  $20.7^\circ$  and  $29.7^\circ$ , *d*-spacings of 7.56, 4.55, 4.37, 4.29 and 3.01 Å, respectively),<sup>33</sup> and were clearly more crystalline (higher  $X_c$ ) than those of CSA-doped MTT1 (Fig. S2, ESI<sup>†</sup> and Table 1) because the presence of the bulky CSA anions interfered with the assembly of the oligoaniline blocks.<sup>12,34</sup> Films of MTT2 were amorphous in both the undoped or CSA-doped state.

The conductance of films of the MTTs were measured as previously reported.<sup>12</sup> Undoped films of tetraaniline-based MTT1 had a conductivity of *ca.*  $1.6 \times 10^{-8}$  S cm<sup>−1</sup>, that was moderately increased by doping with CSA to *ca.*  $2.5 \times 10^{-8}$  S cm<sup>−1</sup> (Table 1). Undoped films of hexaaniline-based MTT2 had a conductivity of *ca.*  $7.3 \times 10^{-8}$  S cm<sup>−1</sup>, that was moderately increased by doping with CSA to *ca.*  $8.6 \times 10^{-8}$  S cm<sup>−1</sup> (Table 1). The higher conductivity of MTT2-based films was because of the greater level of conjugation in the backbone of hexaaniline than in tetraaniline. These conductivities are lower than those of mammalian tissues (typically  $\geq 10^{-4}$  S cm<sup>−1</sup>)<sup>35–37</sup> that should enable the controlled delivery of a drug upon the application of an electrical potential to the EAPs.

We studied the release profiles of the anti-inflammatory drug DMP from MTT films into phosphate buffered saline (PBS) in the absence or presence of an electrical stimulus using the experimental setup depicted in Fig. S3 (ESI<sup>†</sup>). Cyclic voltammograms (Fig. S4, ESI<sup>†</sup>) of the DMP-doped films of MTT1 presented a

**Table 1** Surface and physicochemical properties of the polymer films

	$R_a$ ( $\mu\text{m}$ )	$R_q$ ( $\mu\text{m}$ )	$X_c$ (%)	Conductivity, $\sigma$ (S cm <sup>−1</sup> )
Glass substrate	$0.730 \pm 0.153$	$0.905 \pm 0.182$	N/A <sup>a,b</sup>	N/A
MTT1 undoped	$0.760 \pm 0.299$	$3.272 \pm 6.352$	$68.2^a$	$1.59 \times 10^{-8} \pm 28\%$
MTT1 doped with CSA	$0.760 \pm 0.516$	$1.020 \pm 0.637$	$30.1^a$	$2.49 \times 10^{-8} \pm 33\%$
MTT2 undoped	$0.700 \pm 0.018$	$0.085 \pm 0.024$	$0.0^a$	$7.32 \times 10^{-8} \pm 32\%$
MTT2 doped with CSA	$0.475 \pm 0.009$	$0.060 \pm 0.014$	$0.0^a$	$8.55 \times 10^{-8} \pm 32\%$

<sup>a</sup> As determined by XRD. <sup>b</sup> Not applicable.



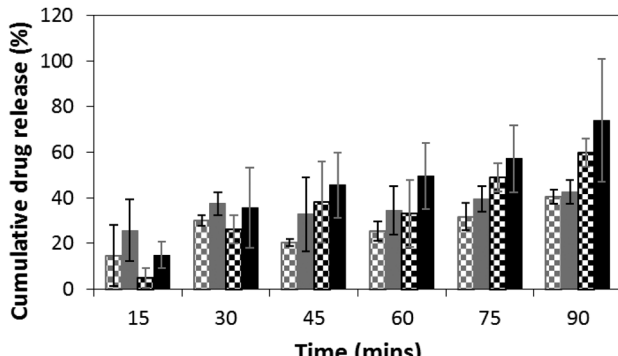


Fig. 2 DMP release from films of MTT1 and MTT2 in the absence and presence of electrical stimulation as determined by UV spectroscopy. MTT1 without electrical stimulation checked grey bars; MTT1 with electrical stimulation solid grey bars; MTT2 without electrical stimulation checked black bars; MTT2 with electrical stimulation solid black bars.

redox process at *ca.* 0.26 V (leucoemeraldine to emeraldine 1 transition), whereas those for MTT2 presented a process at 0.42 V (emeraldine 1 to emeraldine 2 transition), confirming the greater conjugation in the backbone of the longer oligomers (potentials are reported *vs.* a Ag/AgCl reference electrode calibrated with ferrocenemethanol).

We monitored the release of DMP at specific time points spectroscopically, using its characteristic UV absorption at 242 nm. DMP loadings in the films were at 10 wt%. Passive release from films of MTT1 (Fig. 2, grey checked bars) and MTT2 (Fig. 2, black checked bars) was observed, however, release was moderately enhanced by the application of an electrical stimulus (Fig. 2; MTT1 grey bars, MTT2 black bars), typically by 10 to 20% for the first five rounds of stimulation, after which the profiles for MTT1 in the absence/presence of stimulation was observed to be equal which suggests that it is more prone to spontaneous de-doping than the more highly conjugated MTT2. We believe that the release profiles could be improved by tuning both the length of the electroactive oligoaniline, the ratio of electroactive to non-electroactive peptide blocks, and the identity of the non-electroactive peptide (*i.e.* composition and sequence of amino acids).

Analogous electroactive block copolymers incorporating CSA-doped oligoalanines have been shown to support the adhesion of a variety of cells including fibroblasts, keratinocytes, osteoblasts, PC12 cells and Schwann cells.<sup>11</sup> We found that cell viability for the HDFs cultured on the films of MTTs was comparable, and indeed somewhat better than TCP controls (Fig. 3A). However, the adhesion of human dermal fibroblasts (HDFs) to films of undoped or CSA-doped MTT1 was poor by comparison with commercially available Corning Costar<sup>®</sup> tissue culture plate (TCP) controls as determined using the AlamarBlue<sup>®</sup> assay (Fig. 3B), and cells had relatively rounded morphologies indicative of poor cell adhesion (Fig. 4A and B), particularly by comparison with TCP controls (Fig. S5, ESI<sup>†</sup>). Interestingly, HDF adhesion to films of undoped or CSA-doped MTT2 was moderately better, with cells more likely to adopt a spread morphology (Fig. 4C and D). For certain applications, non cell-adhesive biomaterials

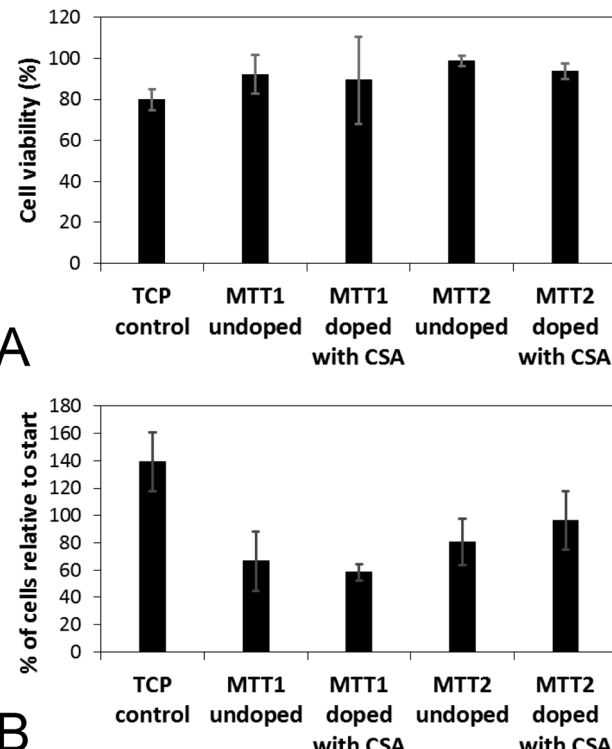


Fig. 3 (A) Assessment of the cell viability of human dermal fibroblasts on various surfaces after 2 days in culture as determined using a LIVE/DEAD<sup>®</sup> Viability/Cytotoxicity Kit. (B) Assessment of cell adhesion on various surfaces after 2 days as determined by the AlamarBlue<sup>®</sup> assay.

are interesting candidates, such as for the manufacture of anti-adhesion membranes;<sup>38</sup> however, for other applications (*e.g.* tissue scaffolds) cell adhesion is beneficial. We believe that cell adhesion could be improved by incorporating cell

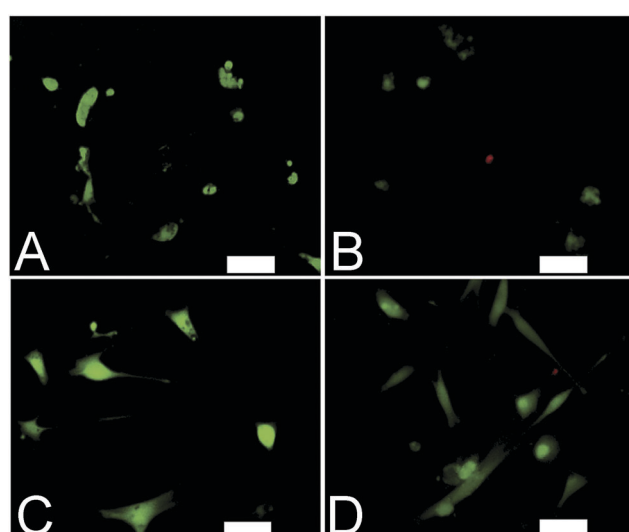


Fig. 4 Adhesion of human dermal fibroblasts on various surfaces after 4 days in culture. (A) Undoped MTT1. (B) CSA-doped MTT1. (C) Undoped MTT2. (D) CSA-doped MTT2. Live cells were stained green by calcein and dead cells were stained red by ethidium using a LIVE/DEAD<sup>®</sup> Viability/Cytotoxicity Kit. Scale bars represent 100  $\mu$ m.



adhesive peptides (*e.g.* the ubiquitous RGD)<sup>10,16,39–41</sup> in the backbone of such EAPs.

## Conclusions

Herein we described electrically-triggered drug release from electroactive molecular tongue-twisters (*i.e.* oligoalanine–oligoaniline–oligoalanine). The electroactive ABA block copolymers based on (A) non-electroactive oligoalanines, and (B) electroactive blocks of oligoanilines, represents a novel platform for drug delivery. The physicochemical properties of the films were characterized by various techniques, and we found that hexaaniline-based MTT2 was more conductive and appeared to be more electrochemically stable towards de-doping than tetraaniline-based MTT1. While HDFs cultured on the surfaces of such films adhered weakly, this could be improved by incorporating cell-adhesive moieties.<sup>39–41</sup> While imperfect, such EAPs represent valuable lead structures for the development of materials that enable us to deliver drugs with clinically relevant chronopharmacologies, and facilitate the treatment of conditions with specific chronobiologies (*e.g.* infectious diseases, pain). We believe that it should be possible to rationally control the release profiles and cell–biomaterial interactions by tuning the length of the electroactive oligoaniline, the ratio of electroactive to non-electroactive peptide blocks, and the identity of the non-electroactive peptide (*i.e.* composition and sequence of amino acids). Specifically, increasing the length of the oligoalanine segments should render them more conductive and electrochemically stable (*i.e.* less likely to be spontaneously de-doped in biological milieu). The composition and sequence of amino acids in the non-electroactive peptide dictate the charge and hydrophobicity of the materials, which play roles in the self-assembly of the peptides (*i.e.* hydrogen bonding interactions, electrostatic interactions) and protein deposition on their surfaces which may be important for cell adhesion. Cell–biomaterial interactions could be controlled through the inclusion of cell-adhesive peptides (*e.g.* RGD, YIGSR, KQAGDV, KHIFSDDSSSE, KRSR),<sup>39–41</sup> and protease-labile domains (APGL, VRN, or indeed oligoalanines such as those in the backbone of MTT1 and MTT2 that are degraded by elastase),<sup>40</sup> potentially facilitate their degradation *in vivo*. Furthermore, molecules with higher ratios of electroactive to non-electroactive peptide blocks should be more conductive, and the inclusion of charged amino acids may facilitate the inclusion of cationic drugs (antibacterials, antiarrhythmics, *etc.*).<sup>42</sup>

## Acknowledgements

We thank Andrea P. Carranza, YoungIn Jun, Jong M. Kim, David J. Mouser, Min Joo Sohn and Pei-Yun Tseng for early work related to the synthesis of well-defined oligomers of aniline, and David Aguilar Jr. and Harrison J. Matthews for assistance with early work related to the drug delivery studies. We thank the University of Texas at Austin for financial support of Jong M. Kim, David J. Mouser and Min Joo Sohn in the form

of Undergraduate Research Fellowships. At the Department of Chemistry at the University of Florida we thank Kari Basso and Louis Searcy for attempts at mass spectrometry analysis. We thank the University of Florida for financial support in the form of startup resources.

## Notes and references

- 1 A. S. Mandal, N. Biswas, K. M. Karim, A. Guha, S. Chatterjee, M. Behera and K. Kuotsu, *J. Controlled Release*, 2010, **147**, 314.
- 2 B. Chertok, M. J. Webber, M. D. Succi and R. Langer, *Mol. Pharmaceutics*, 2013, **10**, 3531.
- 3 M. E. Caldorera-Moore, W. B. Liechty and N. A. Peppas, *Acc. Chem. Res.*, 2011, **44**, 1061.
- 4 P. Leclerc, M. Surin, P. Jonkheijm, O. Henze, A. P. H. J. Schenning, F. Biscarini, A. C. Grimsdale, W. J. Feast, E. W. Meijer, K. Mullen, J. L. Bredas and R. Lazzaroni, *Eur. Polym. J.*, 2004, **40**, 885.
- 5 M. Berggren and A. Richter-Dahlfors, *Adv. Mater.*, 2007, **19**, 3201.
- 6 Z. L. Yue, S. E. Moulton, M. Cook, S. O'Leary and G. G. Wallace, *Adv. Drug Delivery Rev.*, 2013, **65**, 559.
- 7 A. Guiseppi-Elie, *Biomaterials*, 2010, **31**, 2701.
- 8 J. Rivnay, R. M. Owens and G. G. Malliaras, *Chem. Mater.*, 2014, **26**, 679.
- 9 A. D. Bendrea, L. Cianga and I. Cianga, *J. Biomater. Appl.*, 2011, **26**, 3.
- 10 J. G. Hardy, J. Y. Lee and C. E. Schmidt, *Curr. Opin. Biotechnol.*, 2013, **24**, 847.
- 11 B. L. Guo, L. Glavas and A. C. Albertsson, *Prog. Polym. Sci.*, 2013, **38**, 1263.
- 12 J. G. Hardy, D. J. Mouser, N. Arroyo-Currás, S. Geissler, J. K. Chow, L. Nguy, J. M. Kim and C. E. Schmidt, *J. Mater. Chem. B*, 2014, **2**, 6809.
- 13 D. Svirskis, J. Travas-Sejdic, A. Rodgers and S. Garg, *J. Controlled Release*, 2010, **146**, 6.
- 14 V. Pillay, T. S. Tsai, Y. E. Choonara, L. C. du Toit, P. Kumar, G. Modi, D. Naidoo, L. K. Tomar, C. Tyagi and V. M. Ndesendo, *J. Biomed. Mater. Res., Part A*, 2014, **102**, 2039.
- 15 R. Dong, Y. Zhou, X. Huang, X. Zhu X, Y. Lu and J. Shen, *Adv. Mater.*, 2015, **27**, 498.
- 16 A. R. Hirst, B. Escuder, J. F. Miravet and D. K. Smith, *Angew. Chem., Int. Ed.*, 2008, **47**, 8002.
- 17 M. Hasegawa and M. Iyoda, *Chem. Soc. Rev.*, 2010, **39**, 2420.
- 18 S. H. Kim and J. R. Parquette, *Nanoscale*, 2012, **4**, 6940.
- 19 A. J. Hodgson, K. Gilmore, C. Small, G. G. Wallace, I. L. Mackenzie, T. Aoki and N. Ogata, *Supramol. Sci.*, 1994, **1**, 77.
- 20 E. K. Schillinger, E. Mena-Osteritz, J. Hentschel, H. G. Börner and P. Bäuerle, *Adv. Mater.*, 2009, **21**, 1562.
- 21 A. Digennaro, H. Wennemers, G. Joshi, S. Schmid, E. Mena-Osteritz and P. Bäuerle, *Chem. Commun.*, 2013, **49**, 10929.
- 22 Z. Zhang, S. Wei and L. Han, *Adv. Mater. Res.*, 2011, **284–286**, 2110.

23 I. Rozalska, P. Kułyk and I. Kuliszewicz-Bajer, *New J. Chem.*, 2004, **28**, 1235.

24 I. Kuliszewicz-Bajer, I. Rozalska and M. Kurłyk, *New J. Chem.*, 2004, **28**, 669.

25 G. J. M. Habraken, M. Peeters, C. H. J. T. Dietz, C. E. Koninga and A. Heise, *Polym. Chem.*, 2010, **1**, 514.

26 Z. Pang, J. Fu, P. Lv, F. Huang and Q. Wei, *Sensors*, 2014, **14**, 21453.

27 U. Slotta, M. Tammer, F. Kremer, P. Koelsch and T. Scheibel, *Supramol. Chem.*, 2006, **18**, 1.

28 F. Paquet-Mercier, T. Lefevre, M. Auger and M. Pezolet, *Soft Matter*, 2013, **9**, 208.

29 O. S. Rabotyagova, P. Cebe and D. L. Kaplan, *Macromol. Biosci.*, 2010, **10**, 49.

30 J. G. Hardy and T. R. Scheibel, *J. Polym. Sci., Part A: Polym. Chem.*, 2009, **47**, 3957–3963.

31 J. G. Hardy and T. R. Scheibel, *Biochem. Soc. Trans.*, 2009, **37**, 677.

32 J. G. Hardy, A. Leal-Egaña and T. R. Scheibel, *Macromol. Biosci.*, 2013, **13**, 1431.

33 Z. Shao, Z. Yu, J. Hu, S. Chandrasekaran, D. M. Lindsay, Z. Wei and C. F. J. Faul, *J. Mater. Chem.*, 2012, **22**, 16230.

34 Y. Wang, H. D. Tran, L. Liao, X. Duan and R. B. Kaner, *J. Am. Chem. Soc.*, 2010, **132**, 10365.

35 C. Gabriel, S. Gabriel and E. Corthout, *Phys. Med. Biol.*, 1996, **41**, 2231.

36 S. Gabriel, R. W. Lau and C. Gabriel, *Phys. Med. Biol.*, 1996, **41**, 2251.

37 S. Gabriel, R. W. Lau and C. Gabriel, *Phys. Med. Biol.*, 1996, **41**, 2271.

38 P. H. Zeplin, N. C. Maksimovikj, M. C. Jordan, J. Nickel, G. Lang, A. H. Leimer, L. Römer and T. Scheibel, *Adv. Funct. Mater.*, 2014, **24**, 2658.

39 C. Vallejo-Giraldo, A. Kelly and M. J. Biggs, *Drug Discovery Today*, 2014, **19**, 88.

40 H. Shin, S. Jo and A. G. Mikos, *Biomaterials*, 2003, **24**, 4353.

41 K. G. Sreejalekshmi and P. D. Nair, *J. Biomed. Mater. Res., Part A*, 2011, **96A**, 477.

42 K. I. Umehara, T. Iwatsubo, K. Noguchi, T. Usui and H. Kamimura, *Xenobiotica*, 2008, **38**, 1203.

